Geochemical Perspectives Letters

© 2026 The Authors
Published by the European Association of Geochemistry

A revised carbon isotope composition of the convecting upper mantle

J. Shea[1*], J. Maclennan[1], M. Edmonds[1], E. Hughes[2], M. Hartley[3], S. Mikhail[4], M. Perfit[5], O. Shorttle[1,6*]

OPEN ACCESS

https://doi.org/10.7185/geochemlet.2610

Abstract

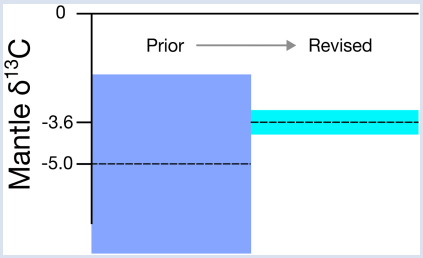

The carbon isotope composition of the convecting upper mantle is key to constraining Earth's carbon budget. Canonical estimates place upper mantle $\delta^{13}C$ between −4 and −6 ‰, but recent measurements suggest inter-ocean basin heterogeneity of several per mille. We test this hypothesis using high precision secondary ion mass spectrometry on olivine hosted melt inclusions from two contrasting settings: mid-ocean ridge basalts from the East Pacific Rise and plume influenced basalts from Iceland's Northern Volcanic Zone. Both melt inclusion suites yield indistinguishable $\delta^{13}C$ compositions despite sampling the upper mantle in different tectonic environments. We propose the convecting upper mantle $\delta^{13}C = -3.6 \pm 0.2$ ‰ (95 % confidence interval; CI), with source heterogeneity present at ±0.8 ‰ (1σ). Use of this new $\delta^{13}C$ value changes the global carbon mass balance and yields a fractional organic carbon burial of $13.7^{+2.3}_{-2.1}$ % (68 % CI), resolving previous discrepancies between isotopic and sedimentary inventory based estimates. Our results have implications for the deep carbon cycle, reducing the need to invoke large carbonate contributions to arc emissions and refining estimates of recycled organic carbon in mantle-derived reservoirs such as diamonds, carbonatites and kimberlites.

Received 21 October 2025 | Accepted 24 February 2026 | Published 7 April 2026

Introduction

The carbon isotope ($\delta^{13}C$) composition of the convecting upper mantle underpins models of core formation, volatile cycles, and bulk silicate Earth (BSE) composition, with implications for carbon budgets and climate (Kump and Arthur, 1999; Wood *et al.*, 2013; Horita and Polyakov, 2015). These calculations rely on indirect proxies sampling distinct mantle reservoirs: peridotitic diamonds (−4.9 ± 1.9 ‰; Stachel *et al.*, 2022) are a metasomatic phase (Cartigny *et al.*, 2014); mantle xenoliths (−5 ‰; Deines, 2002) reflect the lithospheric, not convecting, mantle; and carbonatites (−4.2 ± 2.1 ‰; Moussallam, 2025) record localised heterogeneities rather than typical upper mantle compositions. Direct measurements from un-degassed MORB glasses, such as Mid-Atlantic Ridge (MAR) *'popping rocks'* (~−4 ‰; Javoy and Pineau, 1991; Pineau *et al.*, 2004; Bekaert *et al.*, 2024), provide valuable constraints but depend on accurate accounting for CO_2-rich bubble accumulation, which can decouple bulk carbon isotope compositions from the original melt.

Recent advances in secondary ion mass spectrometry (SIMS) now enable routine $\delta^{13}C$ measurement of olivine hosted melt inclusions, providing direct access to mantle carbon isotope compositions (Lee *et al.*, 2024a; Shea *et al.*, 2025). These inclusions better preserve pre-degassed $\delta^{13}C$ than low pressure quenched glasses, where equilibrium degassing enriches residual melts in ^{12}C as ^{13}C partitions into the vapour phase (Javoy *et al.*, 1978; Mattey *et al.*, 1990; Lee *et al.*, 2024b). Initial applications to natural samples challenge the notion of a homogenous mantle $\delta^{13}C$. Moussallam *et al.* (2025b) reported Pacific upper mantle values ($\delta^{13}C = -8.4 \pm 1.1$ ‰, 1σ) markedly lower than Atlantic values (−3.9 ± 0.4 ‰, 1σ), yet consistent with Southwest Indian Ridge measurements (−7.5 ± 1.4 ‰, 2 s.e.; Moussallam *et al.*, 2025a). Fagradalsfjall melt inclusions (−6.5 ± 2.5 ‰) likewise suggest heterogenous mantle carbon, with local variation (−4 and −9 ‰) implying organic carbon contributions in the Iceland plume (Moussallam *et al.*, 2024). These measurements indicate significant mantle heterogeneity and an average $\delta^{13}C$ lower than the canonical −5 ‰ (Deines, 2002; Stachel *et al.*, 2022).

Previous work has argued that large inter-basin $\delta^{13}C$ heterogeneity may reflect mantle structure, with Pacific subduction zones introducing isotopically light recycled carbon, Atlantic ridges sampling less contaminated mantle, and the Iceland plume carrying variable organic inputs. However, these interpretations rest on small sample data sets (five inclusions for a single location; Moussallam *et al.*, 2025b), and limited CO_2

1. Department of Earth Sciences, University of Cambridge, Cambridge, CB2 3EQ, UK
2. Department of Earth Sciences, University College London, London, WC1E 6BS, UK
3. Department of Earth and Environmental Sciences, University of Manchester, Manchester, M13 9PL, UK
4. School of Earth and Environmental Sciences, University of St Andrews, St Andrews, KY19 9TS, UK
5. Department of Geological Sciences, University of Florida, Gainesville, FL 32611, USA
6. Institute of Astronomy, University of Cambridge, Cambridge, CB3 0HA, UK
* Corresponding authors (emails: jjs83@cam.ac.uk; os258@cam.ac.uk)

concentrations (<250 μg g^{-1} CO_2; Moussallam *et al.*, 2025b). One concern is that this previous work may have captured degassing related fractionation rather than primary mantle $\delta^{13}C$.

We test the null hypothesis that the convecting upper mantle is homogeneous in carbon isotope composition. Using the SIMS protocol of Shea *et al.* (2025), we obtained 85 $\delta^{13}C$ measurements on melt inclusions ($n = 73$), embayments ($n = 6$) and matrix glasses ($n = 6$) from the Siqueiros Transform Fault (East Pacific Rise, EPR) and Borgarhraun (Iceland). Siqueiros represents the primitive end member of the EPR D-MORB (depleted), with minimal fractionation or mixing, whereas Borgarhraun tephra reflect primitive melts from the North Atlantic spreading ridge influenced by the Iceland plume. Their un-degassed melt inclusions define the canonical CO_2/Ba ratio of 100 ± 50 for the convecting mantle (Le Voyer *et al.*, 2017; Hauri *et al.*, 2018; Hirschmann, 2018), underpinning global estimates of mantle carbon content and surface flux *via* melting and degassing (Pacific: Saal *et al.*, 2002; Atlantic: Hauri *et al.*, 2018). Together, these sites can be used to test the Pacific-Atlantic dichotomy in ridge and plume settings. Our samples span 6.38–1678 μg g^{-1} CO_2 and include both mantle-like and degassed CO_2/Ba ratios, allowing independent recognition of degassing modification. We compare melt inclusion results to erupted MORB glass measurements from both the EPR and MAR. Analytical and modelling details are provided in the Supplementary Information.

Results and Discussion

Testing for carbon degassing. CO_2-Ba systematics (Fig. 1) show that despite contrasting petrogenetic histories, which do not bias $\delta^{13}C$ (see SI), Borgarhraun and Siqueiros melt inclusions preserve near-primary volatile compositions, making them ideal for constraining upper mantle $\delta^{13}C$. Inclusions and embayments from both locations have CO_2 concentrations of 36.3–1678 μg g^{-1} and plot along the mantle reference trend (CO_2/Ba = 100 ± 50), indicating minimal pre-entrapment degassing. Carbon undersaturated MORB glasses overlap this trend, confirming it as characteristic of un-degassed spreading ridge melts (Le Voyer *et al.*, 2017; Hirschmann, 2018; Hauri *et al.*, 2018). Most carbon saturated MORB and Icelandic glasses fall to lower CO_2/Ba, reflecting degassing.

Melt inclusion CO_2 concentrations decrease systematically toward matrix glasses (Fig. 2), reflecting progressive volatile loss during ascent and eruption. Borgarhraun matrix glasses show extensive degassing (<10 μg g^{-1} CO_2), typical of subaerial Icelandic lavas (Barry *et al.*, 2014). The most degassed glasses, from Borgarhraun, record the most negative $\delta^{13}C$ values observed in basalts, indicating extreme isotopic fractionation of >99.9 % CO_2 loss (Fig. 2). In contrast, submarine Siqueiros matrix glasses overlap with melt inclusion compositions (Saal *et al.*, 2002), showing they retained volatiles upon eruption. The agreement between melt inclusions and primary CO_2/Ba ratios confirms that our $\delta^{13}C$ data represent upper mantle, not degassing-modified, compositions.

We screened all samples for degassing using statistical outliers and degassing models to ensure $\delta^{13}C$ measurements reflect primary compositions. Weighted mean $\delta^{13}C$ from all melt inclusions embayment at both sites is −3.7 ± 1.6 ‰ (1σ), representing an initial estimate of mantle $\delta^{13}C$. Samples with *z*-scores >3 s.d. were flagged as degassed (red diamonds in Fig. 2). This identified two Borgarhraun and one Siqueiros outlier (<5 % of total data set). Their $\delta^{13}C$ values (range: −7.56 to −8.50 ‰) are systematically lower and contain intermediate CO_2 concentrations that align with partial open system equilibrium degassing trajectories (Fig. 2), confirming partial carbon loss; these were excluded. Siqueiros matrix glasses and Borgarhraun embayments show $\delta^{13}C$-CO_2 consistent with melt inclusions, representing the final pre-eruptive magma recharge, and are retained as primary values.

Carbon isotope homogeneity across ocean basins. Following filtering of degassed melt inclusions, Borgarhraun samples yield a weighted mean $\delta^{13}C = -3.52 \pm 0.12$ ‰ ($n = 47$), while Siqueiros samples yield $\delta^{13}C = -3.66 \pm 0.22$ ‰ ($n = 31$). Although these means differ by 0.14 ‰, this offset is smaller than the standard error of the difference (~0.25 ‰), indicating statistical indistinguishability. The 95 % confidence intervals (Borgarhraun, −3.76 to −3.28 ‰; Siqueiros, −4.10 to −3.22 ‰)

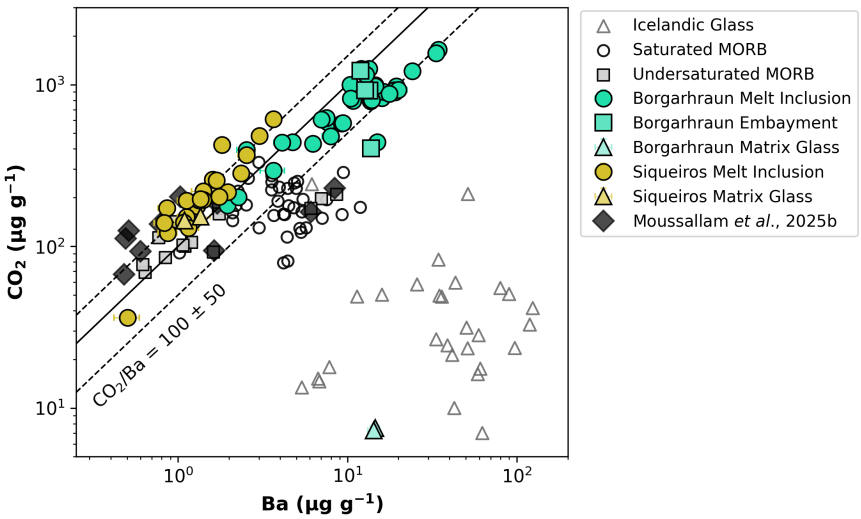

Figure 1 Test for carbon saturation using CO_2 *versus* Ba. Carbon undersaturated melts define CO_2/Ba = 100 ± 50, consistent with undersaturated mantle values prior to degassing. Borgarhraun and Siqueiros melt inclusions and embayments plot within this range, overlapping carbon undersaturated MORB, whereas carbon saturated MORB define higher CO_2/Ba. Siqueiros matrix glasses plot within mantle values; however, Borgarhraun matrix glasses show significant degassing, consistent with other Icelandic glasses that plot at lower CO_2 for a given Ba. Additional MORB glasses from Moussallam *et al.* (2025b) and Icelandic literature data (Barry *et al.*, 2014; Marshall *et al.*, 2024) are shown for comparison.

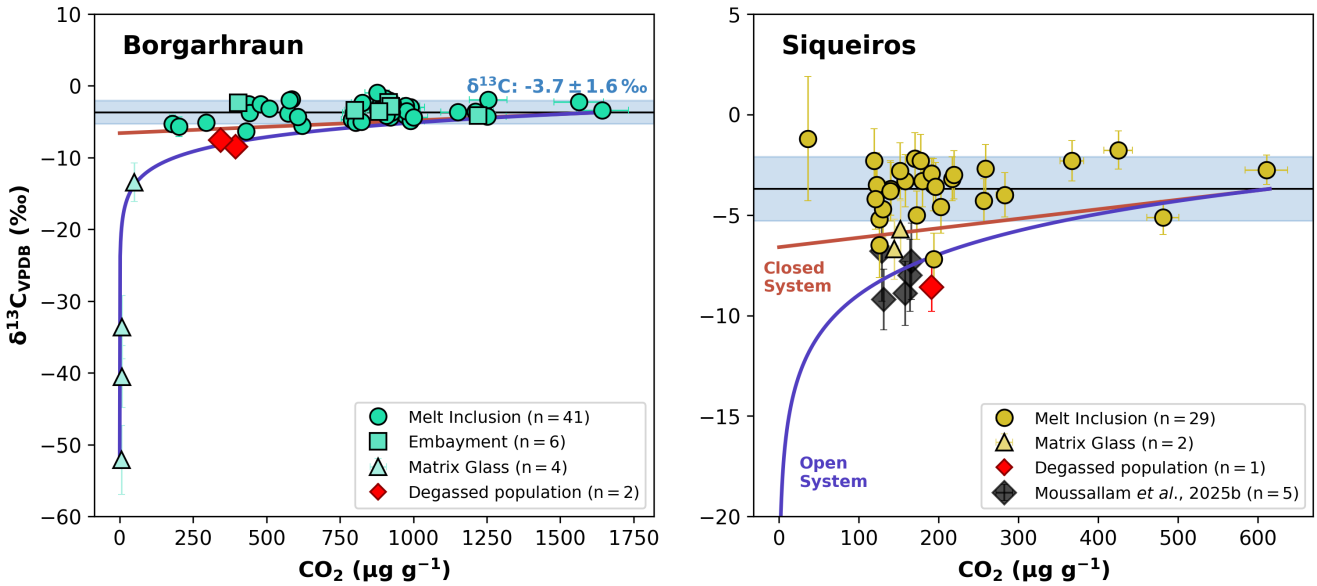

Figure 2 Testing for degassed compositions in Borgarhraun (left) and Siqueiros (right). Melt inclusions (circles), embayments (squares), and matrix glass (triangles) are shown; red diamonds indicate degassed outliers ($|z| > 3$; see SI). Closed and open system degassing curves (brown, purple) use a fractionation factor of +2.9 ‰ (Lee *et al.*, 2024a) and initial mantle $\delta^{13}C$ of −3.7 ± 1.6 ‰ (black line, blue shading), with initial CO_2 from the highest melt inclusion concentrations. Black diamonds show Siqueiros melt inclusion data from Moussallam *et al.* (2025b). Uncertainties are 1σ.

show substantial overlap, with a common range spanning 0.54 ‰. This overlap encompasses most of both uncertainty ranges, confirming that any apparent difference between the locations reflects analytical uncertainty rather than genuine source heterogeneity.

Inverse variance weighting of both data sets yields a combined constraint of $\delta^{13}C = -3.6 \pm 0.2$ ‰ (95 % CI, $n = 78$; Fig. 3; see SI for further details). This analysis yields the most precise estimate of the carbon isotopic composition of the upper mantle yet obtained. The weighting favours Borgarhraun (76 %) due to its superior individual-sample measurement precision, but both locations contribute meaningfully to the final constraint.

Mantle source heterogeneity. Un-degassed melt inclusions reveal significant over dispersion beyond analytical uncertainties: z-score standard deviations are $\sigma_z = 1.40$ (95 % CI; 1.10–1.8) for Borgarhraun, and $\sigma_z = 1.05$ (95 % CI; 0.83–1.4) for Siqueiros. Combined data yield $\sigma_z = 1.26$ (95 % CI; 1.10–1.5), indicating excess variance relative to analytical uncertainty. Over dispersion ($\sigma_z > 1$) indicates isotopic heterogeneity within mantle sources. Individual melt batches captured by melt

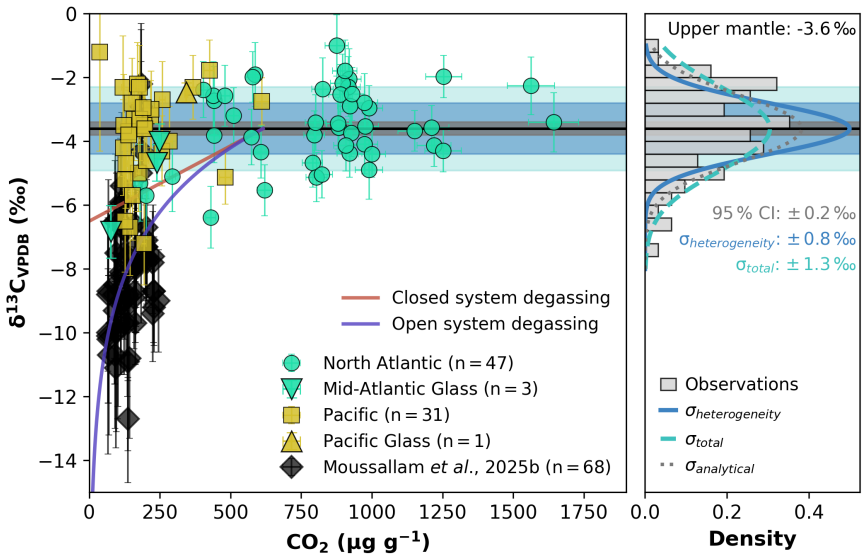

Figure 3 $\delta^{13}C$ (‰ VPDB) *versus* CO_2 (μg g^{-1}) for un-degassed, olivine hosted melt inclusions and new glass measurements from the Atlantic and Pacific compared to literature data from Moussallam *et al.* (2025b). The solid black line shows the preferred convecting upper mantle value (−3.6 ‰), with shaded bands showing the 95 % confidence interval (±0.2 ‰; grey), intrinsic mantle heterogeneity ($\sigma_{heterogeneity}$ = ± 0.8 ‰; blue), and expected observed scatter including analytical uncertainty (σ_{total} = ± 1.3 ‰; teal). Degassing curves show equilibrium closed and open system fractionation trajectories. The right panel shows the $\delta^{13}C$ distribution of un-degassed melt inclusions with Gaussian curves illustrating analytical, heterogeneity, and total variance components. Uncertainty bars are 1σ.

inclusions and embayments preserve isotopically distinct mantle signatures that are otherwise homogenised during substantial mixing in the magma chamber. Variance decomposition quantifies this natural mantle heterogeneity at 0.8 ‰ (1σ; SI). Melt inclusions sample melts that have undergone partial mixing during melt transport and storage, which reduces compositional variance. Therefore, this value likely represents a minimum estimate of intrinsic variability in the convecting mantle.

The coexistence of a consistent mean $\delta^{13}C$ with local scale heterogeneity reflects mantle convection dynamics: sufficiently vigorous for mingling of mantle sources, yet incomplete enough to preserve short length-scale isotopic variability. The upper mantle is stirred, but not mixed, by diffusive homogenisation, so preserves isotopic heterogeneity inherent to melting domains within a larger homogenous mantle that maintains long length-scale bulk compositions. We recommend $\delta^{13}C = -3.6 \pm 0.2$ ‰ (95 % CI) as the convecting upper mantle mean, with 0.8 ‰ (1σ) natural heterogeneity.

Our proposed $\delta^{13}C$ value is supported by measurements of additional MORB glasses: a Pacific glass (East Pacific Rise, ALV981-R23; Shea *et al.*, 2025) and three MAR glasses reported here (CH98-DR02, CH98-DR12 and CH98-DR17). Two MAR glasses erupted at depth (4185 and 4300 m) and overlap with the mantle heterogeneity range of our convecting upper mantle value. In contrast, a third MAR glass contains a low CO_2 (76.8 μg g^{-1} CO_2) and lower $\delta^{13}C$ (-6.8 ± 0.8 ‰), consistent with extensive equilibrium degassing associated with its shallower eruption depth (1800 m). Similarly, the MORB glass data set of Moussallam *et al.* (2025b) spans the mantle heterogeneity range at higher CO_2 concentrations but includes many samples with lower $\delta^{13}C$ and CO_2, consistent with degassing of MORB melts during ascent rather than reflecting primary mantle composition (Fig. 3).

Previously reported MORB glasses (Moussallam *et al.*, 2025a) include many degassed samples that, if treated as primary, bias mantle $\delta^{13}C$ estimates toward lower values. In contrast, our constraint (-3.6 ± 0.2 ‰) closely matches the pristine *'popping rock'* MORB glass (−3.36 ‰; Bekaert *et al.*, 2024). While indirect proxies such as peridotitic diamonds (-4.9 ± 1.9 ‰), mantle xenoliths (~−5 ‰), and carbonatites (-4.2 ± 2.1 ‰) span broad and poorly constrained ranges that partly overlap our estimate; they sample distinct mantle reservoirs rather than the convecting upper mantle accessed by spreading ridge magmatism.

Basis for broad $\delta^{13}C$ homogeneity in the convecting upper mantle. Isotopic uniformity across spreading ridges reflects efficient mantle convection operating on time scales (10^6–10^7 years; Coltice and Schmalzl, 2006) shorter than carbon's mantle residence time (>1 Gyr to ~4.6 Gyr; Dasgupta and Hirschmann, 2010), ensuring effective homogenisation of isotope heterogeneities from subduction zones. Carbon's chemical behaviour further facilitates homogenisation; it depresses the mantle solidus, has strong incompatibility, and shows high silicate melt solubility, promoting redistribution and mixing by incipient melting across large mantle volumes (Green and Wallace, 1988; Ni and Keppler, 2013; Rosenthal *et al.*, 2015). At depth, redox melting during decompression driven breakdown of carbon-bearing phases creates carbonatite melts that remain mobile even at very low melt fractions (<1 wt. %; Rohrbach and Schmidt, 2011; Minarik and Watson, 1995). This property of carbonate melts facilitates efficient isotopic equilibrium. Carbon's long residence time and its chemical behaviour promotes homogenisation of long length-scale variation in the convecting upper mantle.

Carbon cycle implications. Our constraint on the convecting upper mantle $\delta^{13}C$ (-3.6 ± 0.2 ‰) represents a ~1.3 ‰ shift toward more positive values from widely used canonical estimates of −4 to −6 ‰, with broad implications for carbon cycling between Earth's reservoirs. This heavier mantle carbon composition requires revision of BSE carbon budgets and affects global mass balance calculations, from subduction input to volcanic output fluxes, which anchor carbon atmospheric fluxes. Incorporating natural mantle heterogeneity (0.8 ‰, 1σ), a population mean primary magmatic $\delta^{13}C$ value lower than −4.4 ‰ (mean minus 1σ natural heterogeneity) likely indicates recycled contributions, shifting the threshold for recycled carbon input from −6 ‰ to −4.4 ‰.

The mean $\delta^{13}C$ of melt inclusions from mantle derived melts should scatter within the 0.8 ‰ inherent heterogeneity of the −3.6 ‰ mantle mean, providing a baseline for distinguishing primary melt compositions, potentially degassed magmas, or contributions from recycled carbon components. Using previously established -4.9 ± 1.9 ‰ mantle estimates from diamonds, 69 % of diamonds were classified as sampling solely mantle derived carbon (Cartigny *et al.*, 2014; Stachel *et al.*, 2022). Within the framework of this mass balance, our constraint suggests instead that most diamonds are consistent with contributions from ^{13}C-depleted recycled organic carbon: peridotitic diamonds (average $\delta^{13}C = -4.9 \pm 1.9$ ‰) reflect convecting mantle carbon with minor recycled contributions, whereas asthenospheric and transition zone diamonds (-9.4 ± 6.7 ‰) and lower mantle diamonds (-14.5 ± 7.2 ‰) record recycled organic carbon subducted into Earth's deep interior (Stachel *et al.*, 2022). This either reflects a strong bias in the sampling of sub-lithospheric diamonds, a more carbon-poor deep Earth, or diamond formation being internalised within deeply subducted slabs and therefore low mantle carbon contributions. Many carbonatites ($\delta^{13}C = -4.2 \pm 2.1$ ‰; Moussallam, 2025) are consistent with melting of the convecting mantle. Kimberlites and associated melts span a wide $\delta^{13}C$ (range −1.2 to −10.8 ‰, average -5.2 ± 1.2 ‰, 1σ; Giuliani *et al.*, 2025), most consistent with melting of the convecting mantle followed by degassing rather than by melting a mantle source modified by organic or crustal carbonate assimilation (Fig. S-3).

Our revised mantle $\delta^{13}C$ value enables more accurate quantification of volcanic degassing and volatile fluxes. Mason *et al.* (2017) attributed elevated volcanic arc gas $\delta^{13}C$ values (−3.8 to −4.6 ‰) in comparison to a MORB source (−6.0 ‰) to crustal carbonate assimilation. Our baseline, however, suggests these gas values fall within the range of intrinsic mantle heterogeneity, removing the requirement for widespread incorporation of ^{13}C-enriched recycled carbonate or crustal carbonate assimilation in petrogenetic models.

Global carbon cycle mass balance depends on the fraction of organic carbon buried in the solid Earth (f_{org}). We estimate f_{org} using Monte Carlo uncertainty propagation of the standard two end member carbon isotope mass balance (*e.g.*, Derry, 2014):

$$\delta^{13}C_{in} = \delta^{13}C_{org} f_{org} + \delta^{13}C_{carb}(1 - f_{org}),$$

where $\delta^{13}C_{in}$ is the mantle input composition, and $\delta^{13}C_{org}$ and $\delta^{13}C_{carb}$ are the organic and carbonate end members. Using our revised mantle value ($\delta^{13}C_{in} = -3.6 \pm 0.2$ ‰), we obtain $f_{org} = 13.7^{+2.3}_{-2.1}$ % (68 % CI; see SI). This aligns with sedimentary estimates (10–17 %; Derry, 2014) and overlaps, but is lower than, estimates derived from high temperature volcanic gas emissions (15.2 to 18.4 %; Mason *et al.*, 2017).

Previous isotope based estimates of $f_{org} = 19$–34 % assumed mantle carbon isotope compositions of −5 to −6 ‰ using an equivalent mass balance approach (Derry, 2014). Applying the same Monte Carlo framework, using an earlier

mantle value (−4.9 ± 1.9 ‰; Stachel *et al.*, 2022) reproduces similarly elevated burial fractions (Figs. S-5, S-6), demonstrating that the discrepancy arises directly from the assumed mantle isotope composition and its uncertainty. The heavier mantle value determined here resolves this inconsistency and establishes a revised baseline for global carbon cycle mass balance. A lower f_{org} reduces the requirement for long term organic carbon burial to balance mantle degassing *via* volcanism, providing tighter closure on organic burial in Earth's long term carbon cycle.

Conclusions

We establish $\delta^{13}C = -3.6 \pm 0.2$ ‰ as the convecting upper mantle carbon isotope composition, an order of magnitude improvement in precision over previous estimates. This value derives from olivine hosted melt inclusions from distinct spreading ridges: Pacific MORB (Siqueiros Transform Fault) and plume influenced North Atlantic basalts (Borgarhraun, Iceland). Statistical equivalence between these sites (−3.5 ± 0.1 ‰ and −3.7 ± 0.2 ‰), despite ~7000 km separation and contrasting geodynamic settings, indicates large scale isotopic uniformity in bulk mantle, while preserving natural source heterogeneity (0.8 ‰, 1σ) at the melt region scale. Apparent mantle $\delta^{13}C$ heterogeneity in earlier work reflects volatile loss, where CO_2-depleted samples yield systematically lower $\delta^{13}C$ values following degassing trajectories. Such degassed samples artificially bias estimates of mean mantle composition and heterogeneity.

Our revised $\delta^{13}C$ value reframes global carbon cycling. This ~1.3 ‰ shift toward more positive values relative to widely used estimates redefines the recycled carbon threshold to −4.4 ‰, indicating many peridotitic diamonds previously considered mantle derived may contain recycled organic carbon. This baseline also removes the need for substantial crustal carbonate assimilation in volcanic arc gases. Monte Carlo mass balance gives $f_{org} = 13.7^{+2.3}_{-2.1}$ % (68 % CI), consistent with sedimentary inventories (10–17 %) rather than isotopic calculations (19–34 %; Derry, 2014). This value refines end member compositions for global carbon flux models and improves constraints on natural carbon cycle baselines.

Author Contributions and Acknowledgements

JS conceived and led the study, performed SIMS analyses, developed the statistical framework, conducted Monte Carlo modelling, and wrote the manuscript. JM, OS, and ME contributed to study design, interpretation, and manuscript development. EH, MH, SM, and MP contributed to interpretation and manuscript revision. All authors contributed to discussion and approved the final manuscript. We thank Brian Monteleone for expert assistance with SIMS analyses at the Northeast National Ion Microprobe Facility at Woods Hole Oceanographic Institution, operated under the direction of Glenn Gaetani. We thank Iris Buisman for assistance with electron microprobe analyses. We thank Jason Day for assistance with LA-ICP-MS analyses, operated under the direction of Sally Gibson. JS, OS, JM, MH, and SM acknowledge support from UKRI grant NE/V011383/1. JS and OS acknowledge support from the Leverhulme Centre for Life in the Universe Joint Collaborations Research Project Grant G112026/LBAG429. We thank Raúl Fonseca for editorial handling of the manuscript, and David Bekaert and an anonymous reviewer for constructive comments that improved the manuscript.

Editor: Raul O.C. Fonseca

Additional Information

Supplementary Information accompanies this letter at https://www.geochemicalperspectivesletters.org/article2610.

© 2026 The Authors. This work is distributed under the Creative Commons Attribution 4.0 License, which permits unrestricted use, distribution, and reproduction in any medium, provided the original author and source are credited. Additional information is available at http://www.geochemicalperspectivesletters.org/copyright-and-permissions.

Cite this letter as: Shea, J., Maclennan, J., Edmonds, M., Hughes, E., Hartley, M., Mikhail, S., Perfit, M., Shorttle, O. (2026) A revised carbon isotope composition of the convecting upper mantle. *Geochem. Persp. Let.* 39, 36–41. https://doi.org/10.7185/geochemlet.2610

References

Barry, P.H., Hilton, D.R., Füri, E., Halldórsson, S.A., Grönvold, K. (2014) Carbon isotope and abundance systematics of Icelandic geothermal gases, fluids and subglacial basalts with implications for mantle plume-related CO_2 fluxes. *Geochimica et Cosmochimica Acta* 134, 74–99. https://doi.org/10.1016/j.gca.2014.02.038

Bekaert, D.V., Barry, P.H., Curtice, J., Blusztajn, J., Hudak, M., Seltzer, A., Broadley, M.W., Krantz, J.A., Wanless, V.D., Soule, S.A., Mittelstaedt, E., Kurz, M.D. (2024) A carbon, nitrogen, and multi-isotope study of basalt glasses near 14°N on the Mid-Atlantic Ridge. Part A: Degassing processes. *Geochimica et Cosmochimica Acta* 369, 160–178. https://doi.org/10.1016/j.gca.2023.12.015

Cartigny, P., Palot, M., Thomassot, E., Harris, J.W. (2014) Diamond Formation: A Stable Isotope Perspective. *Annual Review of Earth and Planetary Sciences* 42, 699–732. https://doi.org/10.1146/annurev-earth-042711-105259

Coltice, N., Schmalzl, J. (2006) Mixing times in the mantle of the early Earth derived from 2-D and 3-D numerical simulations of convection. *Geophysical Research Letters* 33, L23304. https://doi.org/10.1029/2006GL027707

Dasgupta, R., Hirschmann, M.M. (2010) The deep carbon cycle and melting in Earth's interior. *Earth and Planetary Science Letters* 298, 1–13. https://doi.org/10.1016/j.epsl.2010.06.039

Deines, P. (2002) The carbon isotope geochemistry of mantle xenoliths. *Earth-Science Reviews* 58, 247–278. https://doi.org/10.1016/S0012-8252(02)00064-8

Derry, L.A. (2014) 12.9 - Organic Carbon Cycling and the Lithosphere. In: Holland, H.D., Turekian, K.K. (Eds.) *Treatise on Geochemistry*. Second Edition, Elsevier, Amsterdam, 239–249. https://doi.org/10.1016/B978-0-08-095975-7.01014-7

Giuliani, A., Dalton, H., Pearson, D.G. (2025) Kimberlites: The deepest geochemical probes of Earth. In: Anbar, A., Weis, D. (Eds.) *Treatise on Geochemistry*. Third Edition, Volume 1, Elsevier, Amsterdam, 159–230. https://doi.org/10.1016/B978-0-323-99762-1.00064-4

Green, D.H., Wallace, M.E. (1988) Mantle metasomatism by ephemeral carbonatite melts. *Nature* 336, 459–462. https://doi.org/10.1038/336459a0

Hauri, E.H., Maclennan, J., McKenzie, D., Gronvold, K., Oskarsson, N., Shimizu, N. (2018) CO_2 content beneath northern Iceland and the variability of mantle carbon. *Geology* 46, 55–58. https://doi.org/10.1130/G39413.1

Hirschmann, M.M. (2018) Comparative deep Earth volatile cycles: The case for C recycling from exosphere/mantle fractionation of major (H_2O, C, N) volatiles and from H_2O/Ce, CO_2/Ba, and CO_2/Nb exosphere ratios. *Earth and Planetary Science Letters* 502, 262–273. https://doi.org/10.1016/j.epsl.2018.08.023

Horita, J., Polyakov, V.B. (2015) Carbon-bearing iron phases and the carbon isotope composition of the deep Earth. *Proceedings of the National Academy of Sciences* 112, 31–36. https://doi.org/10.1073/pnas.1401782112

Javoy, M., Pineau, F. (1991) The volatiles record of a "popping" rock from the Mid-Atlantic Ridge at 14°N: chemical and isotopic composition of gas trapped in the vesicles. *Earth and Planetary Science Letters* 107, 598–611. https://doi.org/10.1016/0012-821X(91)90104-P

Javoy, M., Pineau, F., Iiyama, I. (1978) Experimental determination of the isotopic fractionation between gaseous CO_2 and carbon dissolved in tholeiitic

magma. A preliminary study. *Contributions to Mineralogy and Petrology* 67, 35–39. https://doi.org/10.1007/BF00371631

Kump, L.R., Arthur, M.A. (1999) Interpreting carbon-isotope excursions: carbonates and organic matter. *Chemical Geology* 161, 181–198. https://doi.org/10.1016/S0009-2541(99)00086-8

Le Voyer, M., Kelley, K.A., Cottrell, E., Hauri, E.H. (2017) Heterogeneity in mantle carbon content from CO_2-undersaturated basalts. *Nature Communications* 8, 14062. https://doi.org/10.1038/ncomms14062

Lee, H., Moussallam, Y., Aubaud, C., Iacono-Marziano, G., Hammond, K., Ebel, D. (2024a) Carbon isotope fractionation between CO_2 and carbon in silicate melts at high temperature. *Geochimica et Cosmochimica Acta* 380, 208–219. https://doi.org/10.1016/j.gca.2024.07.015

Lee, H., Moussallam, Y., Rose Koga, E.F., Piani, L., Villeneuve, J., Bouden, N., Gurenko, A.A., Monteleone, B., Gaetani, G.A. (2024b) High-precision determination of carbon stable isotope in silicate glasses by secondary ion mass spectrometry: Evaluation of international reference materials. *Chemical Geology* 670, 122428. https://doi.org/10.1016/j.chemgeo.2024.122428

Marshall, E.W., Halldórsson, S.A., Tian, L., Jackson, M.G., Jenner, F., Stefánsson, A. (2024) The effect of diffusion on lithium isotope ratios in Icelandic basalts. *Chemical Geology* 662, 122206. https://doi.org/10.1016/j.chemgeo.2024.122206

Mason, E., Edmonds, M., Turchyn, A.V. (2017) Remobilization of crustal carbon may dominate volcanic arc emissions. *Science* 357, 290–294. https://doi.org/10.1126/science.aan5049

Mattey, D.P., Taylor, W.R., Green, D.H., Pillinger, C.T. (1990) Carbon isotopic fractionation between CO_2 vapour, silicate and carbonate melts: an experimental study to 30 kbar. *Contributions to Mineralogy and Petrology* 104, 492–505. https://doi.org/10.1007/BF01575626

Minarik, W.G., Watson, E.B. (1995) Interconnectivity of carbonate melt at low melt fraction. *Earth and Planetary Science Letters* 133, 423–437. https://doi.org/10.1016/0012-821X(95)00085-Q

Moussallam, Y. (2025) Carbon Isotopes in Magmatic Systems: Measurements, Interpretations, and the Carbon Isotopic Signature of the Earth's Mantle. *Geosciences* 15, 266. https://doi.org/10.3390/geosciences15070266

Moussallam, Y., Rose-Koga, E.F., Fischer, T.P., Georgeais, G., Lee, H.J., Birnbaum, J., Pfeffer, M.A., Barnie, T., Regis, E. (2024) Kinetic Isotopic Degassing of CO_2 During the 2021 Fagradalsfjall Eruption and the $\delta^{13}C$ Signature of the Icelandic Mantle. *Geochemistry, Geophysics, Geosystems* 25, e2024GC011997. https://doi.org/10.1029/2024GC011997

Moussallam, Y., Koga, K.T., Rose-Koga, E.F., Aubaud, C., Lee, H.J., Georgeais, G. (2025a) The carbon isotopic signature of the upper mantle is heterogeneous. *Communications Earth & Environment* 6, 6. https://doi.org/10.1038/s43247-024-01973-9

Moussallam, Y., Rose-Koga, E.F., Aubaud, C., Georgeais, G., Cartigny, P., Koga, K.T., Devidal, J.-L., Michael, P.J., Shimizu, K., Saal, A.E. (2025b) Enigmatic carbon isotopic variability in the oceanic upper mantle. *Proceedings of the National Academy of Sciences* 122, e2502886122. https://doi.org/10.1073/pnas.2502886122

Ni, H., Keppler, H. (2013) Carbon in Silicate Melts. *Reviews in Mineralogy and Geochemistry* 75, 251–287. https://doi.org/10.2138/rmg.2013.75.9

Pineau, F., Shilobreeva, S., Hekinian, R., Bideau, D., Javoy, M. (2004) Deep-sea explosive activity on the Mid-Atlantic Ridge near 34°50′N: a stable isotope (C, H, O) study. *Chemical Geology* 211, 159–175. https://doi.org/10.1016/j.chemgeo.2004.06.029

Rohrbach, A., Schmidt, M.W. (2011) Redox freezing and melting in the Earth's deep mantle resulting from carbon–iron redox coupling. *Nature* 472, 209–212. https://doi.org/10.1038/nature09899

Rosenthal, A., Hauri, E.H., Hirschmann, M.M. (2015) Experimental determination of C, F, and H partitioning between mantle minerals and carbonated basalt, CO_2/Ba and CO_2/Nb systematics of partial melting, and the CO_2 contents of basaltic source regions. *Earth and Planetary Science Letters* 412, 77–87. https://doi.org/10.1016/j.epsl.2014.11.044

Saal, A.E., Hauri, E.H., Langmuir, C.H., Perfit, M.R. (2002) Vapour undersaturation in primitive mid-ocean-ridge basalt and the volatile content of Earth's upper mantle. *Nature* 419, 451–455. https://doi.org/10.1038/nature01073

Shea, J., Hughes, E., Balzer, R., Bindeman, I., Blundy, J., Brooker, R., Botcharnikov, R., Cartigny, P., EIMF, Gaetani, G., Kilgour, G., Maclennan, J., Monteleone, B., Neave, D.A., Shortle, O. (2025) Improved Precision and Reference Materials for Stable Carbon Isotope Measurement in Basaltic Glasses using Secondary Ion Mass Spectrometry. *Geostandards and Geoanalytical Research* 49, 607–627. https://doi.org/10.1111/ggr.12610

Stachel, T., Cartigny, P., Chacko, T., Pearson, D.G. (2022) Carbon and Nitrogen in Mantle-Derived Diamonds. *Reviews in Mineralogy and Geochemistry* 88, 809–875. https://doi.org/10.2138/rmg.2022.88.15

Wood, B.J., Li, J., Shahar, A. (2013) Carbon in the Core: Its Influence on the Properties of Core and Mantle. *Reviews in Mineralogy and Geochemistry* 75, 231–250. https://doi.org/10.2138/rmg.2013.75.8